www.lajss.org
Latin American Journal of Solids and Structures 3 (2006) 279–299

Effect of composite type and its configuration on buckling strength of thin laminated composite plates

M. Kamruzzaman, A. Umar, S. Q. A. Naqvi and N. A. Siddiqui*

Department of Civil Engineering, Aligarh Muslim University, Aligarh, 202002, India

Abstract

For civil engineering applications, a plate which is strong enough against buckling is always desirable. In the market there are number of composites available which differ from each other in various aspects of engineering properties. In the present study, an effort has been made to identify better configuration of given composite to achieve higher buckling strength for laminated anti-symmetric cross and angle-ply simply supported rectangular orthotropic plates subjected to uniaxial compressive loads. The study has further been extended with number of available composites to find the more effective type of composite against buckling for given configuration of laminated plates. For this purpose, a brief formulation, available in the literature, for the estimation of buckling load for orthotropic laminated composite plates has been presented. Based on this formulation a computer program is developed and using this program various parametric studies are conducted to achieve the above objectives.

1 Introduction

Laminated composite plates have been widely used in engineering applications due to their excellent high strength-to-weight ratio, modulus-to-weight ratio, and the controllability of the structural properties with the variation of fiber orientation and the lamina number. However, in such applications, buckling phenomenon was often observed due to the small thickness of composite laminates. Buckling phenomenon is critically dangerous to structural components because the buckling of composite plates usually occurs at a lower applied stress and generates large deformation.

In the recent past, some good works appeared in various journals and conferences proceeding on buckling analysis of composite plates. Chattopadhyay and Gu [1] presented an exact elasticity solution for the buckling of a simply supported orthotropic plate whose behavior was referred to as cylindrical bending. Gu and Chattopadhyay [2] presented three-dimensional elasticity solutions for the buckling of simply supported orthotropic and laminated composite plates. Shukla and Nath [7] analyzed the buckling and post-buckling behavior of the moderately thick angle-ply laminated composite rectangular plates. Khdeir [6] investigated the stability of antisymmetric angle-ply laminated plates. Veres and Kollar [8] presented closed form approximate formulas for

*Corresp. author email: nadeemahsan@rediffmail.com Received 10 Sep 2005; In revised form 14 Aug 2006

Nomenclature

a, b, t	Plate dimensions
m, n	Number of half sine waves in X- and Y-directions respectively
N_x	Applied in plane uni-axial load
$\bar{N}_x$	Critical buckling load
K	Non-dimensional buckling load
u, v, w	Displacements of the plate along X-, Y-, $Z-$directions
∂u^0, ∂v^0, ∂w	Variations in deformation
S1, S3	Simply supported edge in the direction of loading
S2, S4	Simply supported edge in the transverse direction of loading
$\partial M_x, \partial M_y$	Variation in moments
$\partial N_x, \partial N_y, \partial N_{xy}$	Variation in forces

the calculation of rectangular orthotropic plates with clamped and/or simply supported edges. Kamruzzaman et al. [5] studied the buckling behavior of rectangular anti-symmetric laminated composite plates subjected to uniaxial compressive loads.

A detailed review of literature shows that although considerable research work has been done on mechanics of buckling problem in composite plates, a detailed parametric study to identify better configuration and type of composite for civil engineering applications is missing. Keeping this point in view, in the present study, an effort has been made to identify better configuration of given composite to achieve higher buckling strength for laminated anti-symmetric cross and angle-ply simply supported rectangular orthotropic plates subjected to uni-axial compressive loads. The study has further been extended with number of available composites to find the more effective type of composite against buckling for given configuration of laminated plates. For this purpose, a brief formulation, available in the literature, for the estimation of buckling load for orthotropic laminated composite plates has been presented. Based on this formulation a computer program is developed and using this program various parametric studies are conducted to achieve the above objectives.

2 Mathematical formulation

The formulation presented in this section, with some little modification, is based on Classical Lamination Theory, CLT [4]. To use this theory and derive expressions of buckling load for thin orthotropic antisymmetric cross-ply and angle-ply laminated plates, following assumptions have been made:

- The plate thickness is very small compared to its length (a) and width (b) (Fig. 1).
- The plate is made up of perfectly bonded laminae.

- The bonds are infinitesimally thin and no lamina can slip relative to the other. This implies that the displacements are continuous across the lamina boundaries. As a result, the laminate behaves like a lamina with special properties.
- No body force exists.
- Stresses acting in the xy plane (the plane of the plate) dominate the plate behavior. The stresses σ_z, τ_{xz} and τ_{yz} are assumed to be zero such that an approximate state of plane stress is said to exist (wherein only σ_x, σ_y, and τ_{xy} are considered).
- Displacements u, v, and w in X, Y, and Z –directions are small compared to the plate thickness.
- Strains $\varepsilon_x, \varepsilon_y$,and $\gamma_{xy}$are small compared to unity.
- Rotary inertia terms are negligible.

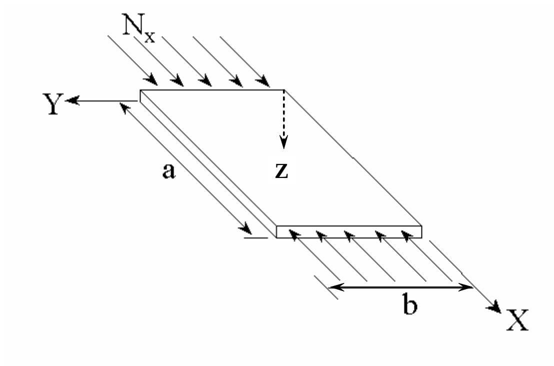

Figure 1: A simply supported laminated rectangular plate under in-plane uniaxial compression

2.1 Governing equations for buckling load

Classical Laminate Theory, CLT [4] has been used to derive the governing buckling equations for a plate subjected to inplane load. To derive the governing equations we have considered first the equilibrium of force and then the equilibrium of moment in a way as discussed below:

The equilibrium equations in terms of the forces (Fig. 2) are

$$\frac{\partial N_x}{\partial x} + \frac{\partial N_{xy}}{\partial y} = 0, \tag{1}$$

$$\frac{\partial N_{xy}}{\partial x} + \frac{\partial N_y}{\partial y} = 0. \tag{2}$$

where N_x, N_y, and N_{xy} are the internal forces in normal and tangential direction.

Again, the equilibrium equation in terms of the moments (Fig. 3) is

$$\frac{\partial^2 M_x}{\partial x^2} + 2\frac{\partial^2 M_{xy}}{\partial x \partial y} + \frac{\partial^2 M_y}{\partial y^2} + N_x \frac{\partial^2 w}{\partial x^2} + N_y \frac{\partial^2 w}{\partial y^2} + 2N_{xy}\frac{\partial^2 w}{\partial x \partial y} = 0, \tag{3}$$

where, N_x, N_y, N_{xy} are the forces applied at the edges.

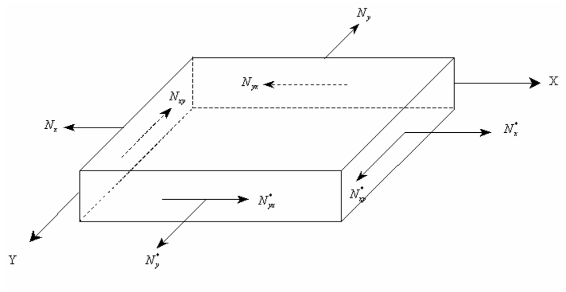

Figure 2: Inplane forces on a laminate

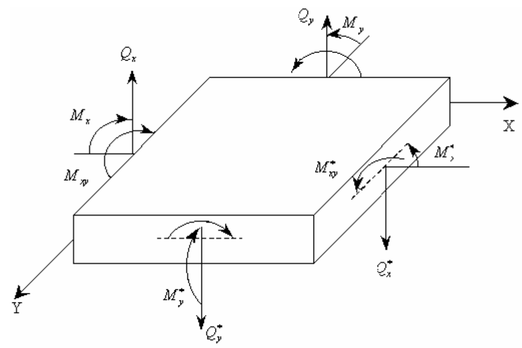

Figure 3: Moments on a laminate

The resultant forces N_x, N_y and N_{xy} and moments M_x, M_y and M_{xy} acting on a laminate are obtained by integration of the stress in each layer or lamina through the laminate thickness. Knowing the stress in terms of the displacement, we can obtain the stress resultants

$N_x, N_y, N_{xy}, M_x, M_y$, and M_{xy}. The stress resultants are defined as

$$N_x = \int_{-\frac{t}{2}}^{\frac{t}{2}} \sigma_x dz, \qquad N_y = \int_{-\frac{t}{2}}^{\frac{t}{2}} \sigma_y dz, \qquad N_{xy} = \int_{-\frac{t}{2}}^{\frac{t}{2}} \tau_{xy} dz,$$
$$M_x = \int_{-\frac{t}{2}}^{\frac{t}{2}} \sigma_x z dz, \qquad M_y = \int_{-\frac{t}{2}}^{\frac{t}{2}} \sigma_y z dz, \qquad M_{xy} = \int_{-\frac{t}{2}}^{\frac{t}{2}} \tau_{xy} z dz. \tag{4}$$

where σ_x, σ_y and τ_{xy} are normal and shear stress.

Actually, N_x, N_y and N_{xy} are the force per unit length of the cross section of the laminate as shown in Fig. 1. Similarly, M_x, M_y, and M_{xy} are the moment per unit length as shown in Fig. 3. Thus, the forces and moments for an N-layer laminate can be defined as

$$\begin{Bmatrix} N_x \\ N_y \\ N_{xy} \end{Bmatrix} = \int_{-\frac{h}{2}}^{\frac{h}{2}} \begin{Bmatrix} \sigma_x \\ \sigma_y \\ \tau_{xy} \end{Bmatrix}_r dz = \sum_{r=1}^{N} \int_{z_{r-1}}^{z_r} \begin{Bmatrix} \sigma_x \\ \sigma_y \\ \tau_{xy} \end{Bmatrix}_r dz, \tag{5}$$

$$\begin{Bmatrix} M_x \\ M_y \\ M_{xy} \end{Bmatrix} = \int_{-\frac{h}{2}}^{\frac{h}{2}} \begin{Bmatrix} \sigma_x \\ \sigma_y \\ \tau_{xy} \end{Bmatrix}_r zdz = \sum_{r=1}^{N} \int_{z_{r-1}}^{z_r} \begin{Bmatrix} \sigma_x \\ \sigma_y \\ \tau_{xy} \end{Bmatrix}_r zdz, \tag{6}$$

where, z_r and z_{r-1} are as defined in Fig. 4. Note that$z_0 = -t/2$. Substituting for σ_x,σ_y,and τ_{xy} in equations (5) and (6) and integrating over the thickness of each layer and adding the results so obtained for N layers, we can write the stress resultants as

$$\begin{Bmatrix} N_x \\ N_y \\ N_{xy} \end{Bmatrix} = \begin{bmatrix} A_{11} & A_{12} & A_{16} \\ A_{12} & A_{22} & A_{26} \\ A_{16} & A_{26} & A_{66} \end{bmatrix} \begin{Bmatrix} \varepsilon_x^0 \\ \varepsilon_y^0 \\ \gamma_{xy}^0 \end{Bmatrix} + \begin{bmatrix} B_{11} & B_{12} & B_{16} \\ B_{12} & B_{22} & B_{26} \\ B_{16} & B_{26} & B_{66} \end{bmatrix} \begin{Bmatrix} k_x \\ k_y \\ k_{xy} \end{Bmatrix}, \tag{7}$$

$$\begin{Bmatrix} M_x \\ M_y \\ M_{xy} \end{Bmatrix} = \begin{bmatrix} B_{11} & B_{12} & B_{16} \\ B_{12} & B_{22} & B_{26} \\ B_{16} & B_{26} & B_{66} \end{bmatrix} \begin{Bmatrix} \varepsilon_x^0 \\ \varepsilon_y^0 \\ \gamma_{xy}^0 \end{Bmatrix} + \begin{bmatrix} D_{11} & D_{12} & D_{16} \\ D_{12} & D_{22} & D_{26} \\ D_{16} & D_{26} & D_{66} \end{bmatrix} \begin{Bmatrix} k_x \\ k_y \\ k_{xy} \end{Bmatrix}, \tag{8}$$

where

$$A_{ij} = \sum_{r=1}^{N} \left(\bar{Q}_{ij}\right)_r (z_r - z_{r-1}),$$
$$B_{ij} = \frac{1}{2} \sum_{r=1}^{N} \left(\bar{Q}_{ij}\right)_r \left(z_r^2 - z_{r-1}^2\right), \tag{9}$$
$$D_{ij} = \frac{1}{3} \sum_{r=1}^{N} \left(\bar{Q}_{ij}\right)_r \left(z_r^3 - z_{r-1}^3\right).$$

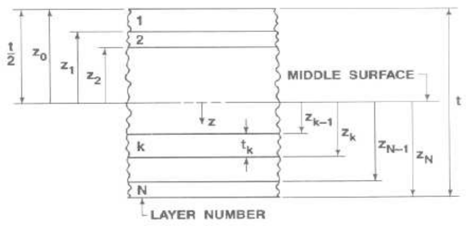

Figure 4: Geometry of an N-layered laminate

Here, A_{ij} are the extensional stiffness, B_{ij} the coupling stiffness, and D_{ij} the flexural stiffness.

For antisymmetric angle-ply and cross-ply laminates stress resultants are simplified in the following sections:

2.1.1 Angle-ply laminates

In the case of angle-ply laminates where the fibre orientation θ alternates from lamina to lamina as$+\theta/-\theta/+\theta/-\theta$, the force and moment resultants are

$$\left\{\begin{array}{c} N_x \\ N_y \\ N_{xy} \end{array}\right\} = \left[\begin{array}{ccc} A_{11} & A_{12} & 0 \\ A_{12} & A_{22} & 0 \\ 0 & 0 & A_{66} \end{array}\right] \left\{\begin{array}{c} \varepsilon_x^0 \\ \varepsilon_y^0 \\ \gamma_{xy}^0 \end{array}\right\} + \left[\begin{array}{ccc} B_{11} & B_{12} & B_{16} \\ B_{12} & B_{22} & B_{26} \\ B_{16} & B_{26} & B_{66} \end{array}\right] \left\{\begin{array}{c} k_x \\ k_y \\ k_{xy} \end{array}\right\}, \quad (10)$$

$$\left\{\begin{array}{c} M_x \\ M_y \\ M_{xy} \end{array}\right\} = \left[\begin{array}{ccc} B_{11} & B_{12} & B_{16} \\ B_{12} & B_{22} & B_{26} \\ B_{16} & B_{26} & B_{66} \end{array}\right] \left\{\begin{array}{c} \varepsilon_x^o \\ \varepsilon_y^0 \\ \gamma_{xy}^0 \end{array}\right\} + \left[\begin{array}{ccc} D_{11} & D_{12} & D_{16} \\ D_{12} & D_{22} & D_{26} \\ D_{16} & D_{26} & D_{66} \end{array}\right] \left\{\begin{array}{c} k_x \\ k_y \\ k_{xy} \end{array}\right\}. \quad (11)$$

Such a laminate is called an *antisymmetric angle-ply laminate.* In this type of laminate, if each lamina has the same thickness, it is then called a *regular antisymmetric angle-ply laminate.* For such a laminate, equations (8) and (9) reduce to

$$\left\{\begin{array}{c} N_x \\ N_y \\ N_{xy} \end{array}\right\} = \left[\begin{array}{ccc} A_{11} & A_{12} & 0 \\ A_{12} & A_{22} & 0 \\ 0 & 0 & A_{66} \end{array}\right] \left\{\begin{array}{c} \varepsilon_x^0 \\ \varepsilon_y^0 \\ \gamma_{xy}^0 \end{array}\right\} + \left[\begin{array}{ccc} 0 & 0 & B_{16} \\ 0 & 0 & B_{26} \\ B_{16} & B_{26} & 0 \end{array}\right] \left\{\begin{array}{c} k_x \\ k_y \\ k_{xy} \end{array}\right\}, \quad (12)$$

$$\left\{\begin{array}{c} M_x \\ M_y \\ M_{xy} \end{array}\right\} = \left[\begin{array}{ccc} 0 & 0 & B_{16} \\ 0 & 0 & B_{26} \\ B_{16} & B_{26} & 0 \end{array}\right] \left\{\begin{array}{c} \varepsilon_x^0 \\ \varepsilon_y^0 \\ \gamma_{xy}^0 \end{array}\right\} + \left[\begin{array}{ccc} D_{11} & D_{12} & 0 \\ D_{12} & D_{22} & 0 \\ 0 & 0 & D_{66} \end{array}\right] \left\{\begin{array}{c} k_x \\ k_y \\ k_{xy} \end{array}\right\}, \quad (13)$$

2.1.2 Cross-ply Laminates

There is yet another class of laminates. Here the laminae are oriented alternatively at 0^0 and 90^0. A laminate of this type is termed as a cross-ply laminate. Such a laminate can, again, be either symmetric cross-ply or antisymmetric cross-ply.

Substituting for $N_x, N_y, N_{xy}, M_x, M_y, M_{xy}$ from equations (10) and (11), after substituting for $\varepsilon_x^0, \varepsilon_y^0, \gamma_{xy}^0, k_x, k_y, k_{xy}$ [4], in equations (1), (2), and (3), we get the governing equations as

$$\begin{aligned} &A_{11}\frac{\partial^2 u^0}{\partial x^2} + (A_{12}+A_{66})\frac{\partial^2 v^0}{\partial x \partial y} + A_{16}(\frac{\partial^2 v^0}{\partial x^2} + 2\frac{\partial^2 u^0}{\partial x \partial y}) + A_{26}\frac{\partial^2 v^0}{\partial y^2} + A_{66}\frac{\partial^2 u^0}{\partial y^2} \\ &-B_{11}\frac{\partial^3 w}{\partial x^3} - 3B_{16}\frac{\partial^3 w}{\partial x^2 \partial y} - (B_{12}+2B_{66})\frac{\partial^3 w}{\partial x \partial y^2} - B_{26}\frac{\partial^3 w}{\partial y^3} = 0, \end{aligned} \tag{14a}$$

$$\begin{aligned} &A_{16}\frac{\partial^2 u^0}{\partial x^2} + (A_{12}+A_{66})\frac{\partial^2 u^0}{\partial x \partial y} + A_{26}\frac{\partial^2 u^0}{\partial y^2} + A_{66}\frac{\partial^2 v^0}{\partial x^2} + 2A_{26}\frac{\partial^2 v^0}{\partial x \partial y} + A_{22}\frac{\partial^2 v^0}{\partial y^2} \\ &B_{16}\frac{\partial^3 w}{\partial x^3} - (B_{12}+2B_{66})\frac{\partial^3 w}{\partial x^2 \partial y} - 3B_{26}\frac{\partial^3 w}{\partial x \partial y^2} - B_{22}\frac{\partial^3 w}{\partial y^3} = 0, \end{aligned} \tag{14b}$$

$$\begin{aligned} &D_{11}\frac{\partial^4 w}{\partial x^4} + 4D_{16}\frac{\partial^4 w}{\partial x^3 \partial y} + (2D_{12}+4D_{66})\frac{\partial^4 w}{\partial x^2 \partial y^2} + 4D_{26}\frac{\partial^4 w}{\partial x \partial y^3} + D_{22}\frac{\partial^4 w}{\partial y^4} \\ &-B_{11}\frac{\partial^3 u^0}{\partial x^3} - 3B_{16}\frac{\partial^3 u^0}{\partial x^2 \partial y} - (B_{12}+2B_{66})\frac{\partial^3 u^0}{\partial x \partial y^2} - B_{26}\frac{\partial^3 u^0}{\partial y^3} - B_{16}\frac{\partial^3 v^0}{\partial x^3} \\ &-(B_{12}+2B_{66})\frac{\partial^3 v^0}{\partial x \partial y^2} - B_{22}\frac{\partial^3 v^0}{\partial y^3} = -N_x\frac{\partial^2 w}{\partial x^2} - N_y\frac{\partial^2 w}{\partial y^2} - 2N_{xy}\frac{\partial^2 w}{\partial x \partial y}. \end{aligned} \tag{14c}$$

For a general laminate, all the above three equations, i.e., equations (14), have to be solved simultaneously as they are coupled. In the present study, we shall consider only simply supported antisymmetric laminated plates. For such simply supported composite plates, these equations are simplified and their closed-form solutions are obtained, as discussed in the following section.

2.2 Buckling load for simply supported laminated plates

Consider the general class of laminated rectangular plates that are simply supported along edges x = 0, x = a, y = 0, and y = b and subjected to uniform in-plane force in the x-direction as shown in Fig. 1. With this boundary condition, the buckling load has been determined separately for antisymmetric cross-ply and antisymmetric angle-ply laminates and presented below:

2.2.1 Antisymmetric cross-ply laminates

Antisymmetric cross-ply laminates have extensional stiffnesses $A_{11}, A_{12}, A_{22} = A_{11}$ and A_{66}, coupling stiffnesses $B_{11}$and $B_{22} = -B_{11}$, and flexural stiffnesses $D_{11}, D_{12}, D_{22} = D_{11}$ and D_{66}. Because of this bending-extension coupling, the $N_x, N_y, N_{xy}, M_x, M_y$and M_{xy} reduce to the following coupled buckling differential equations:

$$A_{11}\frac{\partial^2 u^0}{\partial x^2} + (A_{12}+A_{66})\frac{\partial^2 v^0}{\partial x \partial y} + A_{66}\frac{\partial^2 u^0}{\partial y^2} - B_{11}\frac{\partial^3 w}{\partial x^3} = 0, \tag{15}$$

$$(A_{12}+A_{66})\frac{\partial^2 u^0}{\partial x \partial y} + A_{66}\frac{\partial^2 v^0}{\partial y^2} + A_{11}\frac{\partial^2 v^0}{\partial y^2} + B_{11}\frac{\partial^3 w}{\partial y^3} = 0, \tag{16}$$

$$D_{11}\left(\frac{\partial^4 w}{\partial x^4}+\frac{\partial^4 w}{\partial y^4}\right)+2\left(D_{12}+2D_{66}\right)\frac{\partial^4 w}{\partial x^2\partial y^2}-B_{11}\left(\frac{\partial^3 u^0}{\partial x^3}-\frac{\partial^3 v^0}{\partial y^3}\right)+N_x\frac{\partial^2 w}{\partial x^2}=0. \quad (17)$$

To solve the problem for simply supported edge boundary condition S2 [3]:

$$\text{at } x=0,a: \qquad \partial w=0, \quad \partial M_x=B_{11}\frac{\partial u^0}{\partial x}-D_{11}\frac{\partial^2 w}{\partial x^2}-D_{12}\frac{\partial^2 w}{\partial y^2}=0, \quad (18)$$

$$\partial v^0=0, \quad \partial N_x=A_{11}\frac{\partial u^0}{\partial x}+A_{12}\frac{\partial v^0}{\partial y}-B_{11}\frac{\partial^2 w}{\partial x^2}=0. \quad (19)$$

$$\text{at } y=0,b: \qquad \partial w=0, \quad \partial M_y=-B_{11}\frac{\partial v^0}{\partial y}-D_{12}\frac{\partial^2 w}{\partial x^2}-D_{11}\frac{\partial^2 w}{\partial y^2}=0, \quad (20)$$

$$\partial u^0=0, \quad \partial N_y=A_{12}\frac{\partial u^0}{\partial x}+A_{11}\frac{\partial v^0}{\partial y}+B_{11}\frac{\partial^2 w}{\partial y^2}=0. \quad (21)$$

A solution of the type

$$\begin{aligned}
\partial u^0 &= \bar{u}\cos\frac{m\pi x}{a}\sin\frac{n\pi y}{b},\\
\partial v^0 &= \bar{v}\sin\frac{m\pi x}{a}\cos\frac{n\pi y}{b},\\
\partial w &= \bar{w}\sin\frac{m\pi x}{a}\cos\frac{n\pi y}{b}.
\end{aligned} \quad (22)$$

satisfy the above boundary conditions and the governing differential equations exactly if (Jones [4]):

$$\bar{N}_x=\left(\frac{a}{m\pi}\right)^2\left(T_{33}+\frac{2T_{12}T_{23}T_{13}-T_{22}T_{13}^2-T_{11}T_{23}^2}{T_{11}T_{22}-T_{12}^2}\right), \quad (23)$$

where,

$$\begin{aligned}
T_{11} &= A_{11}\left(\frac{m\pi}{a}\right)^2+A_{66}\left(\frac{n\pi}{b}\right)^2,\\
T_{12} &= \left(A_{12}+A_{66}\right)\left(\frac{m\pi}{a}\right)\left(\frac{n\pi}{b}\right),\\
T_{13} &= -B_{11}\left(\frac{m\pi}{a}\right)^3,\\
T_{22} &= A_{11}\left(\frac{n\pi}{b}\right)^2+A_{66}\left(\frac{m\pi}{a}\right)^2,\\
T_{23} &= B_{11}\left(\frac{n\pi}{b}\right)^3,\\
T_{33} &= D_{11}\left[\left(\frac{m\pi}{a}\right)^4+\left(\frac{n\pi}{b}\right)^4\right]+2\left(D_{12}+2D_{66}\right)\left(\frac{m\pi}{a}\right)^2\left(\frac{n\pi}{b}\right)^2.
\end{aligned} \quad (24)$$

The lowest buckling load has been found by a searching procedure involving integer values of m and n. To implement this procedure first for a given value of n (e.g. 1), m was incremented from 1 to 10 (maximum possible value of m) and at every value of m the N_x, given by Eqn. 23, was computed. Thereafter, n was incremented to next higher integer value (e.g. 2) and again for this value of n, m was incremented from 1 to 10 and at every value of n *and* m N_x, was computed. This process was repeated until for all possible combinations of m and n the N_x is known. Having known the all N_x values, the minimum N_x is sorted. This minimum N_x represents the buckling load for a simply supported antisymmetric cross-ply laminate subjected to inplane loading.

2.2.2 Antisymmetric angle-ply laminates

Antisymmetric angle-ply laminates have extensional stiffnesses A_{11}, A_{12}, A_{22} and A_{66}, coupling stiffnesses B_{16} and B_{26}, and flexural stiffnesses D_{11}, D_{12}, D_{22}, and D_{66}. This type of laminate exhibits a different kind of bending-extension coupling than does the antisymmetric cross-ply laminate. The coupled buckling differential equations are

$$A_{11}\frac{\partial^2 u^0}{\partial x^2} + (A_{12}+A_{66})\frac{\partial^2 v^0}{\partial x \partial y} + A_{66}\frac{\partial^2 u^0}{\partial y^2} - 3B_{16}\frac{\partial^3 w}{\partial x^2 \partial y} - B_{26}\frac{\partial^3 w}{\partial y^3} = 0, \tag{25}$$

$$(A_{12}+A_{66})\frac{\partial^2 u^0}{\partial x \partial y} + A_{66}\frac{\partial^2 v^0}{\partial x^2} + A_{22}\frac{\partial^2 v^0}{\partial y^2} - B_{16}\frac{\partial^3 w}{\partial x^3} - 3B_{26}\frac{\partial^3 w}{\partial x \partial y^2} = 0, \tag{26}$$

$$\begin{aligned} &D_{11}\frac{\partial^4 w}{\partial x^4} + 2\left(D_{12}+2D_{66}\right)\frac{\partial^4 w}{\partial x^2 \partial y^2} + D_{22}\frac{\partial^4 w}{\partial y^4} \\ &-B_{16}\left(3\frac{\partial^3 u^0}{\partial^2 x \partial y} + \frac{\partial^3 v^0}{\partial x^3}\right) - B_{16}\left(3\frac{\partial^3 v^0}{\partial x \partial y^2} + \frac{\partial^3 u^0}{\partial y^3}\right) + N_x\frac{\partial^2 w}{\partial x^2} = 0. \end{aligned} \tag{27}$$

To solve the problem for simply supported edge boundary condition S3 (this boundary condition differs significantly from the S2 condition used for antisymmetric cross-ply laminates) [9,10]:

$$\text{at}\, x = 0, a: \qquad \partial w = 0, \qquad \partial M_x = B_{16}\left(\frac{\partial v^0}{\partial x} + \frac{\partial u^0}{\partial y}\right) - D_{11}\frac{\partial^2 w}{\partial x^2} - D_{12}\frac{\partial^2 w}{\partial y^2} = 0, \tag{28}$$

$$\partial u^0 = 0, \qquad \partial N_{xy} = A_{66}\left(\frac{\partial v^0}{\partial x} + \frac{\partial u^0}{\partial y}\right) - A_{16}\frac{\partial^2 w}{\partial x^2} - B_{26}\frac{\partial^2 w}{\partial y^2} = 0. \tag{29}$$

$$\text{at } y = 0, b: \qquad \partial w = 0, \qquad \partial M_y = B_{26}\left(\frac{\partial v^0}{\partial x} + \frac{\partial u^0}{\partial y}\right) - D_{12}\frac{\partial^2 w}{\partial x^2} - D_{22}\frac{\partial^2 w}{\partial y^2} = 0, \tag{30}$$

$$\partial v^0 = 0, \qquad \partial N_{xy} = A_{66}\left(\frac{\partial v^0}{\partial x} + \frac{\partial u^0}{\partial y}\right) - B_{16}\frac{\partial^2 w}{\partial x^2} - B_{26}\frac{\partial^2 w}{\partial y^2} = 0. \tag{31}$$

A solution of the type

$$\begin{aligned}
\partial u^0 &= \bar{u}\sin\frac{m\pi x}{a}\cos\frac{n\pi y}{b}, \\
\partial v^0 &= \bar{v}\cos\frac{m\pi x}{a}\sin\frac{n\pi y}{b}, \\
\partial w &= \bar{w}\sin\frac{m\pi x}{a}\cos\frac{n\pi y}{b}.
\end{aligned} \tag{32}$$

satisfies the above boundary conditions and the governing differential equations exactly if (Jones [4]):

$$\bar{N}_x = \left(\frac{a}{m\pi}\right)^2 \left(T_{33} + \frac{2T_{12}T_{23}T_{13} - T_{22}T_{13}^2 - T_{11}T_{23}^2}{T_{11}T_{22} - T_{12}^2}\right), \tag{33}$$

where

$$\begin{aligned}
T_{11} &= A_{11}\left(\frac{m\pi}{a}\right)^2 + A_{66}\left(\frac{n\pi}{b}\right)^2, \\
T_{12} &= (A_{12} + A_{66})\left(\frac{m\pi}{a}\right)\left(\frac{n\pi}{b}\right), \\
T_{13} &= -\left[3B_{16}\left(\frac{m\pi}{a}\right)^2 + B_{26}\left(\frac{n\pi}{b}\right)^2\right]\left(\frac{n\pi}{b}\right), \\
T_{22} &= A_{22}\left(\frac{n\pi}{b}\right)^2 + A_{66}\left(\frac{m\pi}{a}\right)^2, \\
T_{23} &= -\left[B_{16}\left(\frac{m\pi}{a}\right)^2 + 3B_{26}\left(\frac{n\pi}{b}\right)^2\right]\left(\frac{m\pi}{a}\right), \\
T_{33} &= D_{11}\left(\frac{m\pi}{a}\right)^4 + 2\left(D_{12} + 2D_{66}\right)\left(\frac{m\pi}{a}\right)^2\left(\frac{n\pi}{b}\right)^2 + D_{22}\left(\frac{n\pi}{b}\right)^4.
\end{aligned} \tag{34}$$

Equation (29) represents the buckling load for a simply supported antisymmetric angle-ply laminate subjected to in-plane loading.

3 Results and discussion

To carry out various numerical studies, we have considered a simply supported composite plate which is subjected to inplane uniaxial load N_x on the side 'b' (Fig. 1). To study the effect of various geometric and material parameters on buckling load a single composite, graphite/epoxy (Table 1) has been considered. However, to study the effect of type of composite on buckling load six most common composite laminates have been considered (Table 2).

Using material properties shown in Table 1, buckling load for cross-ply and angle-ply laminates (for $\theta = 0^0, 15^0, 30^0, 45^0 \& 60^0$) have been obtained and shown in Table 3. The analysis has been carried out for a laminated plate having aspect ratio 1, number of layers 4, thickness 5.0 mm, and width as 500 mm. The results presented in the table shows that the magnitude of buckling load is higher for angle-ply composite plate than corresponding cross-ply composite plate. This is due to the fact that in cross-ply laminated plate every alternate fiber is oriented perpendicular to the direction of the applied load and fibers have very small strength in transverse direction. Further, at an angle of 45^0 the buckling load is maximum for the angle-ply laminated plate. This is so because at an angle of 45^0 the stiffness is maximum which gives a higher buckling load. Thus, if cost and other design parameters favour to have higher buckling strength, it is better to have an angle-ply laminated plate with lamination angle of 45^0.

Table 1: Engineering properties of graphite/epoxy

Type of fiber	E_T (kN/mm^2)	E_L/E_T	G_L/G_T	ν_{LT}	ν_{TL}
Graphite/epoxy	11.0	40.0	0.5	0.25	0.25

Table 2: Engineering properties of different composites

Type of fiber	Designated	E_L (kN/mm^2)	E_T (kN/mm^2)	G_{LT} (kN/mm^2)	ν_{LT}	ν_{TL}
Random short fiber	C1	10.89	7.58	2.48	0.22	0.22
Graphite/epoxy (Type1)	C2	172.36	6.89	3.45	0.25	0.25
Boron/epoxy	C3	206.84	18.61	6.89	0.21	0.21
Graphite/epoxy (Type2)	C4	137.89	14.48	5.86	0.21	0.21
S-glass/epoxy	C5	51.71	11.72	5.52	0.25	0.57
Carbon/epoxy	C6	206.84	5.17	2.59	0.25	0.006

Table 3: Results of the analysis

Buckling load (kN/m)					
Cross-ply	Angle-ply (θ)				
	60	15^0	30^0	45^0	60^0
165.16	197.07	210.039	274.03	308.48	249.89

3.1 Parametric study under single composite

Figures 5 and 6 show the variation of nondimensional buckling load with aspect ratio (p) for graphite/epoxy cross-ply and angle-ply laminated plates. The results are plotted in nondimensional form. For antisymmetric cross-ply laminates nondimensional buckling load has been defined by

$$K = \frac{\bar{N}_x b^2}{\pi^2 D_{22}} \tag{35}$$

where $\bar{N}_x$ is critical buckling load; b is width of plate; D_{22} is transverse flexural stiffness. For, antisymmetric angle-ply laminates, however, nondimensional buckling load has been defined by

$$K = \frac{\bar{N}_x b^2}{E_T t^3} \tag{36}$$

where E_T is transverse elastic modulus; and t is the thickness of laminate.

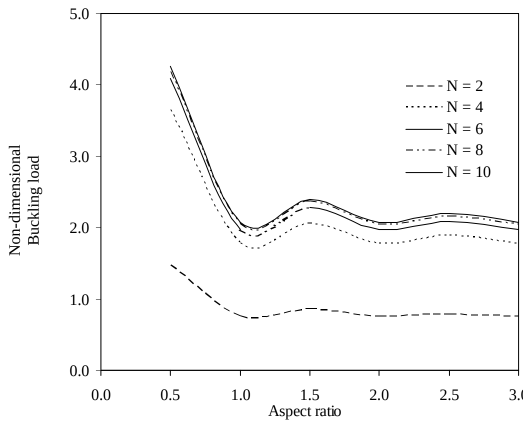

Figure 5: Effect of aspect ratio on buckling load for antisymmetric cross-ply laminates

Graphs show with change in aspect ratio, there is change in buckling load. This is due to the fact that the value of m changes with aspect ratio p ($= a/b$). The effect of aspect ratio is

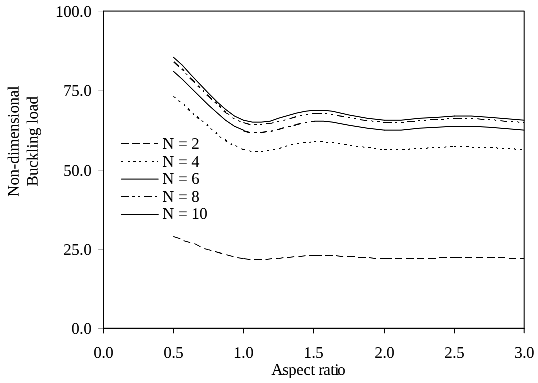

Figure 6: Effect of aspect ratio on buckling load for antisymmetric angle-ply laminates

more pronounced if p is less than 1.5. However, its effect diminishes beyond 3.0. For $1.5 \leq p \leq 3.0$ the effect is moderate.

Figure 7 shows the variation of nondimensional buckling load as a function of lamination angle for an antisymmetric angle-ply square laminate. Figure shows that the buckling load reaches to its maximum value at $\theta = 45^0$ due to higher stiffness at this angle. It is an established fact that higher stiffness increases the buckling load. The graph also shows that there is a remarkable difference in buckling load between two layered and many layered laminates for all values of θ. This is due to the influence of bending-extension coupling. For two layered plates effect of coupling is considerably high, however, for multilayered plates this effect is insignificant. Further, it is to be noted that the buckling mode along the X-direction has two half sine waves beyond $\theta > 60^0$.

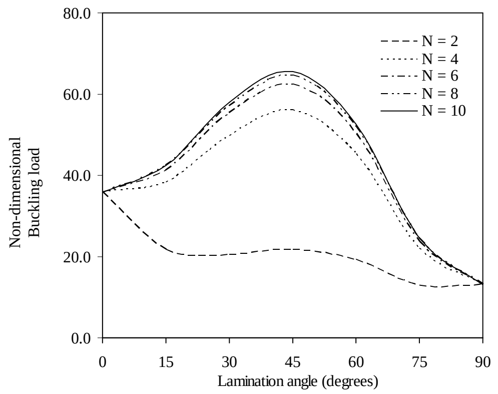

Figure 7: Effect of lamination angle on buckling load for antisymmetric angle-ply laminates

Figures 8 and 9 show the variation of relative uniaxial buckling load $\left(\frac{\bar{N}_x}{\bar{N}_{x_0}}\right)$ as a function of modulus ratio for an antisymmetric cross-ply and angle-ply square laminate made up of

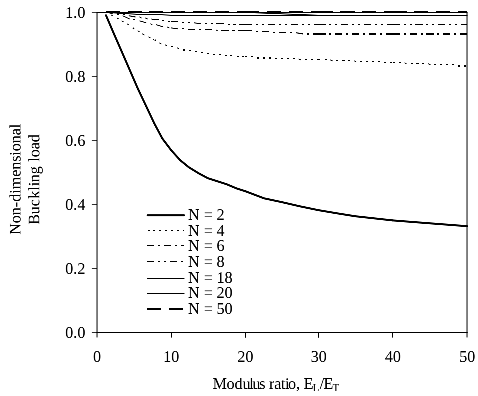

Figure 8: Effect of modulus ratio on buckling load for antisymmetric cross-ply laminates

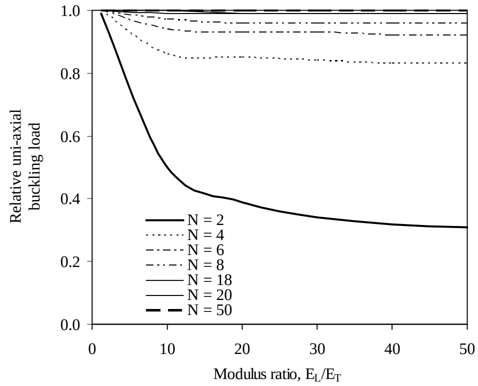

Figure 9: Effect of modulus ratio on buckling load for antisymmetric angle-ply laminates

graphite/epoxy. Here, $\overline{N}_{x_0}$ is the buckling load of an orthotropic plate ($B_{11} = 0$). Figures show that for lesser number of layers (e.g. number of layers = 2, 4), the relative uniaxial buckling load initially decreases sharply with an increase of modulus ratio from 1.25 to 10 and becomes almost constant for significantly high values of modulus ratio (e.g. $E_L/E_T > 10$).

3.2 Parametric Study under Different Composites

Figures 10 and 11 show the variation of buckling load as a function of aspect ratio for an antisymmetric cross-ply and angle-ply laminated plates made up by different composites. It is to be noted that mode number m and n vary with aspect ratio. For the present range of aspect ratio the value of m varies from 1 to 4 but n remains same as 1. From these figures, it is evident that the buckling load for boron/epoxy is maximum and minimum for random short fiber. This is be due to highest longitudinal elastic modulus for boron/epoxy and lowest for random short fiber.

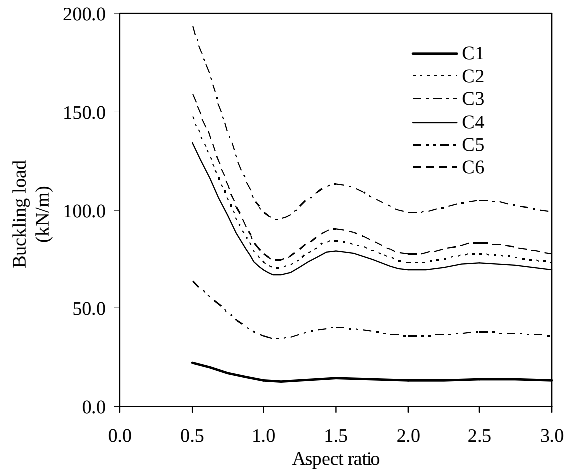

Figure 10: Effect of aspect ratio on buckling load for antisymmetric cross-ply laminated plates
C1-Random short fiber; C2- Graphite/epoxy (Type 1); C3 - Boron/epoxy
C4 - Graphite/epoxy (Type 2); C5 - S-Glass/epoxy; C6 - Carbon/epoxy

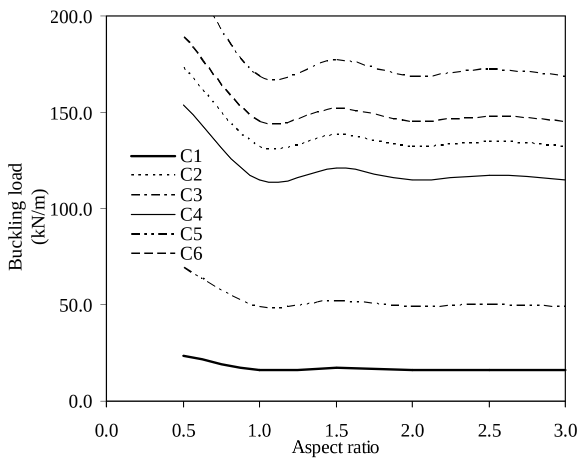

Figure 11: Effect of aspect ratio on buckling load for antisymmetric angle-ply laminated plates
C1-Random short fiber; C2- Graphite/epoxy (Type 1); C3 - Boron/epoxy
C4 - Graphite/epoxy (Type 2); C5 - S-Glass/epoxy; C6 - Carbon/epoxy

Figure 12 shows the effect of lamination angle on buckling load for antisymmetric angle-ply laminated square plate made up of different composites. It is clear from this figure that the variation of buckling load is considerably high for C2, C3, C4 and C6 composites whereas the variation is insignificant for C1 & C5. This is so because for C1 & C5 elastic modulus ratio (E_L/E_T) is close to 1 and for other composites this ratio is quite higher than 1.

Figures 13 and 14 show the variation of buckling load as a function of number of layers for an

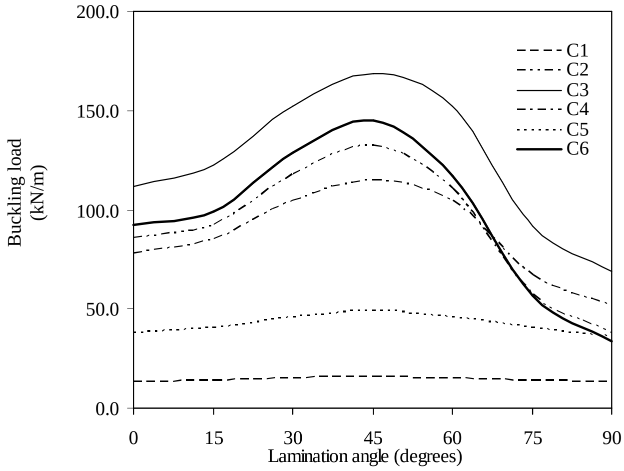

Figure 12: Effect of lamination angle on buckling load for antisymmetric angle-ply laminated plates

C1-Random short fiber; C2- Graphite/epoxy (Type 1); C3 - Boron/epoxy
C4 - Graphite/epoxy (Type 2); C5 - S-Glass/epoxy; C6 - Carbon/epoxy

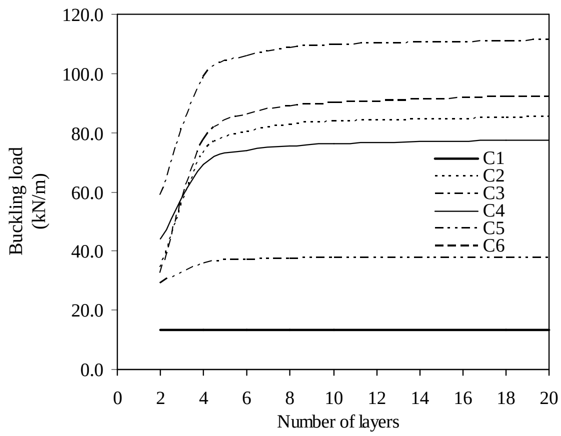

Figure 13: Effect of number of layers on buckling load for antisymmetric cross-ply laminated plates

C1-Random short fiber; C2- Graphite/epoxy (Type 1); C3 - Boron/epoxy
C4 - Graphite/epoxy (Type 2); C5 - S-Glass/epoxy; C6 - Carbon/epoxy

antisymmetric cross-ply and angle-ply laminated square plates made up by different composites. These figure show that the buckling load on a plate of random short fiber do not vary with the variation of number of layers. This is be due to the fact that for random short fiber $E_L/E_T \approx 1$ or in other words plate behave more or less like an isotropic plate. For other composites the buckling load increases as the number of layers increases from 2 to 6. After that the buckling load becomes almost constant. This is due to the fact that the effect of coupling becomes almost negligible for plates having more than 6-layers. It is to noted from these figures that the buckling load is higher in case of angle-ply ($\theta = 45^0$) laminated plate than corresponding cross-ply laminated plate.

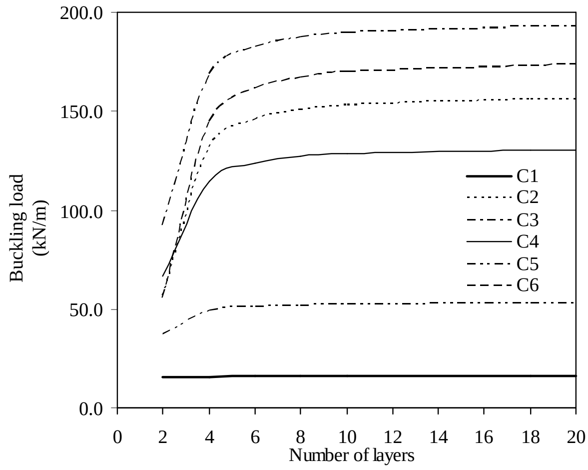

Figure 14: Effect of number of layers on buckling load for antisymmetric angle-ply laminated plates

C1-Random short fiber; C2- Graphite/epoxy (Type 1); C3 - Boron/epoxy
C4 - Graphite/epoxy (Type 2); C5 - S-Glass/epoxy; C6 - Carbon/epoxy

Figures 15 and 16 show the variation of buckling load as a function of thickness for antisymmetric cross-ply and angle-ply laminated square plates made up of different composites. It is clear from the figure that there is dramatic increase in buckling load with increase in laminate thickness. The variation is approximately cubic in nature. This is because buckling load is a function of cube of laminate thickness. Further the buckling load for boron/epoxy is maximum whereas the buckling load for random short fiber is minimum among the six composites considered here for both cross-ply and angle-ply laminated plates. This is due to the fact that the buckling load is more for a composite having more longitudinal elastic modulus.

Figures 17 and 18 show a quantitative comparision of buckling load for various types of composites. Figures show that the highest buckling load is for C3 (boron/epoxy) whereas the lowest buckling load is for C1 (random short fiber). This indicates that if cost is not the main issue it is always better to use boron/epoxy to form a laminated composite plate to resist uniaxial inplane compressive load.

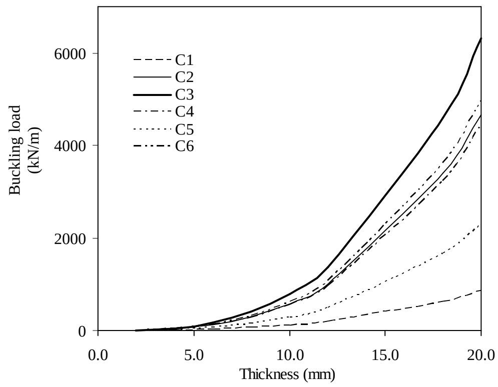

Figure 15: Effect of thickness on buckling load for antisymmetric cross-ply laminated plates C1-Random short fiber; C2- Graphite/epoxy (Type 1); C3 - Boron/epoxy C4 - Graphite/epoxy (Type 2); C5 - S-Glass/epoxy; C6 - Carbon/epoxy

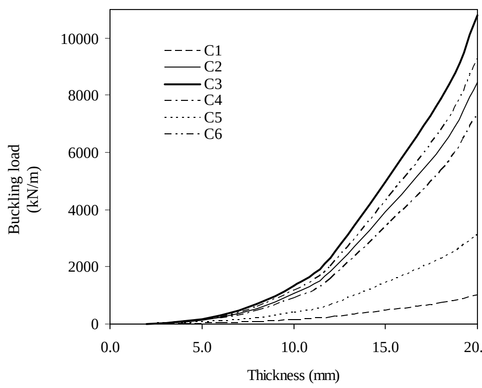

Figure 16: Effect of thickness on buckling load for antisymmetric angle-ply laminated plates C1-Random short fiber; C2- Graphite/epoxy (Type 1); C3 - Boron/epoxy C4 - Graphite/epoxy (Type 2); C5 - S-Glass/epoxy; C6 - Carbon/epoxy

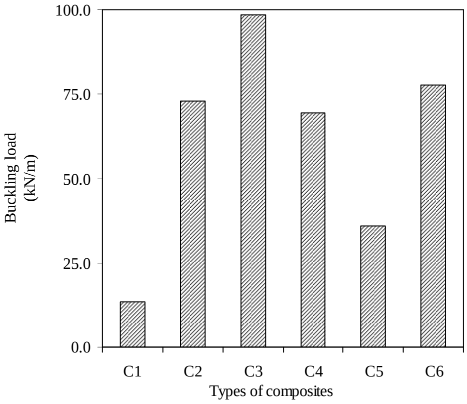

Figure 17: Effect of type of composites on buckling load for antisymmetric cross-ply laminated plates
C1-Random short fiber; C2- Graphite/epoxy (Type 1); C3 - Boron/epoxy
C4 - Graphite/epoxy (Type 2); C5 - S-Glass/epoxy; C6 - Carbon/epoxy

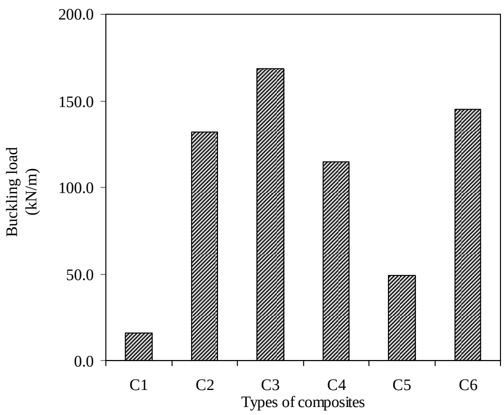

Figure 18: Effect of composites on buckling load for antisymmetric angle-ply laminated plates
C1-Random short fiber; C2- Graphite/epoxy (Type 1); C3 - Boron/epoxy
C4 - Graphite/epoxy (Type 2); C5 - S-Glass/epoxy; C6 - Carbon/epoxy

4 Conclusions

Following conclusions have been drawn from the present parametric study:

1. In general the buckling load for an antisymmetric angle-ply laminated plate is higher than antisymmetric cross-ply laminated plate.
2. Out of the six composites, considered in the present study, the boron/epoxy has the highest and the random short fiber has the lowest magnitudes of buckling load.
3. The coupling effect decreases the magnitude of buckling load. This effect is more dominant for lesser number of layers.
4. There is dramatic increase in buckling load with increase in laminate thickness. The variation is approximately cubic in nature.
5. The buckling load decreases with an increase of aspect ratio (a/b) upto one for both cross-ply and angle-ply laminated plates. However, for aspect ratio greater than one, variation in the buckling load is insignificant.
6. Effect of numbers of layers on buckling load diminishes as the number of layers become more than eight.
7. The variation of buckling load becomes almost constant for higher values of elastic modulus ratio.
8. Composites having higher longitudinal elastic moduli have higher buckling load.
9. For antisymmetric angle-ply laminated plates, the buckling load is maximum at an angle of 45^0.
10. The effect of different parameters (e.g. number of layers, aspect ratio, lamination angle etc.) for random short fiber is almost negligible.

References

[1] A. Chattopadhyay and H. Gu. Exact elasticity solution for buckling of composite laminates. *Composite Structures*, 34(3):291–299, 1996.

[2] H. Gu and A. Chattopadhyay. Three-dimensional elasticity solution for buckling of composite laminates. *Composite Structures*, 50:29–35, 2000.

[3] R.M. Jones. Buckling and vibration of rectangular unsymmetrically laminated cross-ply plates. *AIAA Journal*, pages 1626–1632, December 1973.

[4] R.M. Jones. *Mechanics of Composite Materials*. McGraw-Hill Book Company, 1999.

[5] M. Kamruzzaman, S.Q.A. Naqvi, A. Umar, and N.A. Siddiqui, editors. *Buckling behavior of rectangular antisymmetric laminated plates*, Aligarh, India, April 2005. Department of Civil Engineering, Aligarh Muslim University, Department of Civil Engineering, Aligarh Muslim University. pp. 83-91.

[6] A.A. Khdeir. Stability of antisymmetric angle-ply laminated plates. *Journal of Engineering Mechanics*, 445(5):952–963, 1989.

[7] K.K. Shukla and Y. Nath. Analytical solution for buckling and post-buckling of angle-ply laminated plates under thermomechanical loading. *International Journal of Non-Linear Mechanics*, 36:1097–1108, 2001.

[8] I.A. Veres and L.P. Kollar. Buckling of rectangular orthotropic plates subjected to biaxial normal forces. *Journal of Composite Materials*, 35(7):625–635, 2001.

[9] J.M. Whitney. *A study of the effect of coupling between bending and stretching on the mechanical behavior of layered anisotropic composite materials.* PhD thesis, Department of Engineering Mechanics, The Ohio State University, Columbus, Ohio, 1968.

[10] J.M. Whitney. Bending-extension coupling in laminated plates under transverse loading. *J. Composite Materials*, pages 20–28, January 1969.